Comput Mech
DOI 10.1007/s00466-008-0246-6

ORIGINAL PAPER

The method of fundamental solutions for a biharmonic inverse boundary determination problem

A. Zeb · D. B. Ingham · D. Lesnic

Received: 13 September 2007 / Accepted: 18 January 2008

Abstract In this paper, a nonlinear inverse boundary value problem associated to the biharmonic equation is investigated. This problem consists of determining an unknown boundary portion of a solution domain by using additional data on the remaining known part of the boundary. The method of fundamental solutions (MFS), in combination with the Tikhonov zeroth order regularization technique, are employed. It is shown that the MFS regularization numerical technique produces a stable and accurate numerical solution for an optimal choice of the regularization parameter.

Keywords Biharmonic equation · Inverse problem · Boundary determination · Method of fundamental solutions · Regularization

1 Introduction

The problem of determining an unknown sub-boundary $\gamma \subset \partial\Omega$ of a two-dimensional domain $\Omega \subset \mathbb{R}^2$ is important in many engineering applications, such as a nondestructive evaluation of the material loss caused by corrosion. An example of such an application is the problem of detection of corrosion of complex metallic assemblies in aircraft structures. Clearly, this detection of corrosion has both economic and safe implications, as an early detection of corrosion extends the life of the aircraft structure considerably.

In this paper, we develop a numerical method to determine material loss on an inaccessible, or partially inaccessible, portion γ of the boundary $\partial\Omega$ of a material that occupies an open bounded domain $\Omega \subset \mathbb{R}^2$ in which the biharmonic equation $\nabla^4\psi = 0$ holds. The underlying idea is that we measure the solution ψ and its the normal derivative ψ', and the Laplacian of the solution $\nabla^2\psi = \omega$ and its normal derivative $(\nabla^2\psi)' = \omega'$ on the remaining accessible part of the boundary $\Gamma = \partial\Omega - \gamma$, where the prime $'$ denotes the outward normal derivative. Then we would like to recover the unknown boundary γ, if it exists. On this inaccessible boundary portion γ, the solution ψ is also known. The local existence and uniqueness of such a boundary stems from the existence and uniqueness of the solution of the Cauchy problem for elliptic equations. If one knows the Cauchy data for an elliptic equation then the solution of the equation is uniquely determined [23]. However, the problem is still ill-posed since its solution, if it exists, is not stable under small input data perturbations.

Prior to this study, Lesnic et al. [16] and Marin [17], respectively, proposed a numerical technique to solve inverse Laplace and Helmholtz boundary determination problems in potential corrosion damage. They discretised the problem using the boundary element method (BEM) and solved the resulting nonlinear algebraic equations by minimizing the Tikhonov regularized function. Here, we use the method of fundamental solutions (MFS) to discretise the biharmonic boundary detection problem and generate an equivalent system of nonlinear algebraic equations, by generalizing the approach of [20] for potential (harmonic) corrosion damage.

A. Zeb on study leave visiting the University of Leeds.

A. Zeb
COMSATS Institute of Information Technology,
30 H-8/1, Islamabad, Pakistan

D. B. Ingham
Centre for Computational Fluid Dynamics,
University of Leeds, Leeds LS2 9JT, UK

D. Lesnic (✉)
Department of Applied Mathematics,
University of Leeds, Leeds LS2 9JT, UK
e-mail: amt5ld@maths.leeds.ac.uk

The problem of solving these equations is then reformulated as an unconstrained minimization problem. Since the original problem is ill-posed, the un-regularized minimization procedure produces an unstable and inaccurate numerical solution for the unknown part of the boundary. Therefore, we use the Tikhonov regularization technique to produce an accurate and stable numerical solution.

Both the BEM and the MFS are based on the fundamental solutions of the governing equations being explicitly available and their solution methodologies do not depend upon the interior discretization of computational regions. However, unlike the presence of singular integrals in the BEM, the basic idea of MFS is to decompose the solution of the governing equations by superposition of fundamental solutions with proper intensities. Therefore, the original problem reduces to finding the unknown constant coefficients that multiply the fundamental solutions and the coordinates of the source points such that the approximations satisfy as well as possible the given boundary conditions. Moreover, the MFS locates the source points outside the computational domain. Then, no special treatment of the singularities in the fundamental solutions is required. Hence, the MFS is considered to be a meshless technique that encompasses all the advantages of the boundary methods such as the BEM. One controversial issue regarding the MFS is the location of the source points. However, this problem can be overcome by employing a nonlinear least-squares minimization procedure. Alternatively, the source points can be prescribed a priori and the post-processing analysis of the errors can indicate their optimal location [2,9,18].

The MFS was first proposed by Kurpradze and Aleksidze [15] and its numerical formulation first given by Mathon and Johnston [19]. Since then, the MFS has been successfully used in numerical solutions of the Poisson equation [3,8], diffusion equation [4,27], Helmholtz equation [11,28], biharmonic equation [12–14,22], and Stokes equations [29–31]. The MFS has also been effectively used for solving inverse problems in which some of the ingredients necessary to solve a direct problem are missing, see, e.g. [5,18]. For further details on the MFS the reader is referred to [6,7] and the references therein.

The aim of this paper is to extend the range of applications of the MFS to solve inverse biharmonic boundary detection problems. With this motivation, in Sect. 2 we present the mathematical formulation of the problem. In Sect. 3 we discretise the problem by using the MFS and obtain a system of nonlinear algebraic equations. In Sect. 4, we present some numerical experiments and discuss the results which are stabilized by using a zeroth-order Tikhonov regularization method. Finally, concluding remarks are presented in Sect. 5.

2 Mathematical formulation

The inverse problem we consider consists of the biharmonic equation and the boundary specification of the solution ψ and its normal derivative $\psi^{'}$, and the Laplacian of the solution $\nabla^2\psi = \omega$ and its normal derivative $(\nabla^2\psi)^{'} = \omega^{'}$. We can mathematically state this as follows:

$$\nabla^4\psi(\mathbf{x}) = 0, \qquad \mathbf{x} \in \Omega, \tag{1}$$

$$\psi(\mathbf{x}) = \varphi(\mathbf{x}), \quad \psi^{'}(\mathbf{x}) = \chi(\mathbf{x}), \quad \mathbf{x} \in \Gamma, \tag{2}$$

$$\omega(\mathbf{x}) = \xi(\mathbf{x}), \quad \omega^{'}(\mathbf{x}) = \zeta(\mathbf{x}), \quad \mathbf{x} \in \Gamma. \tag{3}$$

where $\Gamma = \partial\Omega - \gamma$. Then we would like to find the unknown boundary $\gamma \subset \partial\Omega$ from the given Cauchy data (2) and (3) and

$$\psi(\mathbf{x}) = \vartheta(\mathbf{x}), \quad \mathbf{x} \in \gamma, \tag{4}$$

where ϑ is a given function on γ. In this mathematical model, the functions ψ and ω may represent the streamfunction and vorticity in two-dimensional Stokes flows or the deflection and bending moment of a plate in elasticity. Usually, $\vartheta \equiv 0$ in (4), and in this case one needs to determine a perfectly conductive boundary crack γ. Also, instead of prescribing ψ on γ as in (4), we could prescribe the normal derivative $\psi^{'}$ on γ with no major modifications of the analysis.

In general, a solution to the problem (1)–(4) will not exist if the data φ, χ, ξ, ζ and ϑ are prescribed arbitrarily. Certain compatibility conditions need to be satisfied by these data in order to ensure that a solution exists [24]. Further, as mentioned in Sect. 1, the uniqueness of the boundary γ follows from the uniqueness of the solution to the Cauchy problem for elliptic equations [23]. However, due to the mathematically ill-posed nature of the inverse problem given by Eqs. (1)–(4), the stability of the numerical solution for the unknown boundary γ becomes an important issue that is to be addressed in the following sections.

3 The method of fundamental solutions

The fundamental solutions $G(\mathbf{x}, \mathbf{y})$ and $W(\mathbf{x}, \mathbf{y})$ of the two-dimensional biharmonic and Laplace's equations are given by [12],

$$G(\mathbf{x}, \mathbf{y}) = r^2(\mathbf{x}, \mathbf{y}) \ln r(\mathbf{x}, \mathbf{y}), \quad W(\mathbf{x}, \mathbf{y}) = \ln r(\mathbf{x}, \mathbf{y}), \tag{5}$$

respectively, where $r(\mathbf{x}, \mathbf{y}) = |\mathbf{x} - \mathbf{y}|$ denotes the distance between the points $\mathbf{x}$ and $\mathbf{y}$. The MFS approximates the solution $\psi(\mathbf{x})$ of the biharmonic equation (1) by a linear combination of the fundamental solutions $G(\mathbf{x}, \mathbf{y})$ and $W(\mathbf{x}, \mathbf{y})$ with respect to the source points $\mathbf{y}^j \in \mathbb{R}^2 - \overline{\Omega}$, $j = \overline{1, M}$, i.e.,

$$\psi(\mathbf{x}) = \psi^M(\mathbf{c}, \mathbf{d}, \mathbf{Y}, \mathbf{x}) = \sum_{j=1}^{M} \Big[c_j G(\mathbf{x}, \mathbf{y}^j) + d_j W(\mathbf{x}, \mathbf{y}^j) \Big], \quad \mathbf{x} \in \overline{\Omega}, \tag{6}$$

where $\mathbf{c} = [c_1, c_2, \ldots, c_M]$, $\mathbf{d} = [d_1, d_2, \ldots, d_M]$ are vectors of constant coefficients and $\mathbf{Y}$ is a vector with $2M$ components consisting of the two-dimensional coordinates of the M source points $\mathbf{y}^j$. Accordingly, the boundary values of $\psi^{'}$, ω and $\omega^{'}$ can be approximated as follows:

$$\begin{aligned} \psi^{'}(\mathbf{x}) &= \frac{\partial}{\partial n} \Big[\psi^M(\mathbf{c}, \mathbf{d}, \mathbf{Y}, \mathbf{x}) \Big] \\ &= \sum_{j=1}^{M} \Big[c_j G^{'}(\mathbf{x}, \mathbf{y}^j) + d_j W^{'}(\mathbf{x}, \mathbf{y}^j) \Big], \quad \mathbf{x} \in \partial\Omega, \end{aligned} \tag{7}$$

$$\begin{aligned} \omega(\mathbf{x}) &= \nabla^2 \psi^M(\mathbf{c}, \mathbf{d}, \mathbf{Y}, \mathbf{x}) \\ &= \omega^M(\mathbf{c}, \mathbf{d}, \mathbf{Y}, \mathbf{x}) = \sum_{j=1}^{M} c_j Q(\mathbf{x}, \mathbf{y}^j), \quad \mathbf{x} \in \partial\Omega, \end{aligned} \tag{8}$$

$$\omega^{'}(\mathbf{x}) = \frac{\partial}{\partial n} \Big[\omega^M(\mathbf{c}, \mathbf{d}, \mathbf{Y}, \mathbf{x}) \Big] = \sum_{j=1}^{M} c_j Q^{'}(\mathbf{x}, \mathbf{y}^j), \quad \mathbf{x} \in \partial\Omega, \tag{9}$$

where $G^{'}$, $W^{'}$, Q and $Q^{'}$ are given by

$$G^{'}(\mathbf{x}, \mathbf{y}) = \{1/2 + \ln r(\mathbf{x}, \mathbf{y})\} \frac{\partial}{\partial n} \left\{ r^2(\mathbf{x}, \mathbf{y}) \right\}, \quad \mathbf{x} \in \partial\Omega, \quad \mathbf{y} \in \mathbb{R}^2 - \overline{\Omega}, \tag{10}$$

$$W^{'}(\mathbf{x}, \mathbf{y}) = \left\{ \frac{1}{2} \frac{1}{r^2(\mathbf{x}, \mathbf{y})} \right\} \frac{\partial}{\partial n} \left\{ r^2(\mathbf{x}, \mathbf{y}) \right\}, \quad \mathbf{x} \in \partial\Omega, \quad \mathbf{y} \in \mathbb{R}^2 - \overline{\Omega}, \tag{11}$$

$$Q(\mathbf{x}, \mathbf{y}) = 4 \{1 + \ln r(\mathbf{x}, \mathbf{y})\}, \quad \mathbf{x} \in \partial\Omega, \quad \mathbf{y} \in \mathbb{R}^2 - \overline{\Omega}, \tag{12}$$

$$Q^{'}(\mathbf{x}, \mathbf{y}) = \left\{ \frac{2}{r^2(\mathbf{x}, \mathbf{y})} \right\} \frac{\partial}{\partial n} \left\{ r^2(\mathbf{x}, \mathbf{y}) \right\}, \quad \mathbf{x} \in \partial\Omega, \quad \mathbf{y} \in \mathbb{R}^2 - \overline{\Omega}. \tag{13}$$

We choose $N = N_1 + N_2$ collocation points $\mathbf{x}^i$, $i = \overline{1, N}$, on the boundary $\partial\Omega$ such that N_1 points belong to the known boundary Γ on which the over-specified boundary conditions (2) and (3) are prescribed, and N_2 points are on the unknown boundary γ.

The problem defined by (1)–(4) now reduces to solving a system of $4N_1 + N_2$ algebraic equations in $2M + 2N_2$ unknowns

$$\begin{aligned} \mathbb{A}(\mathbf{X}) &:= \begin{pmatrix} G(\mathbf{x}^i, \mathbf{y}^j) & W(\mathbf{x}^i, \mathbf{y}^j) \\ G^{'}(\mathbf{x}^i, \mathbf{y}^j) & W^{'}(\mathbf{x}^i, \mathbf{y}^j) \\ Q(\mathbf{x}^i, \mathbf{y}^j) & 0 \\ Q^{'}(\mathbf{x}^i, \mathbf{y}^j) & 0 \end{pmatrix} \begin{pmatrix} c_j \\ d_j \end{pmatrix} \\ &= \begin{pmatrix} \psi(\mathbf{x}^i), \ i = \overline{1, N} \\ \chi(\mathbf{x}^i), \ i = \overline{1, N_1} \\ \xi(\mathbf{x}^i), \ i = \overline{1, N_1} \\ \zeta(\mathbf{x}^i), \ i = \overline{1, N_1} \end{pmatrix} =: \mathbf{b}, \end{aligned} \tag{14}$$

where $j = \overline{1, M}$ and the repeated index j in the left hand side of Eq. (14) is assumed to be summed over. In the right-hand side of (14), $\psi(\mathbf{x}^i) = \varphi(\mathbf{x}^i)$ for $i = \overline{1, N_1}$, and $\psi(\mathbf{x}^i) = \vartheta(\mathbf{x}^i)$ for $i = \overline{(N_1 + 1), N}$.

Since N_2 points $\mathbf{x}^i$ for $i = \overline{(N_1 + 1), N}$ lie on the unknown boundary γ, the coefficient matrix $\mathbb{A}$ has entries which are dependent upon the unknown coordinates of the points on the boundary portion γ. Thus the expression (14) represents a system of nonlinear algebraic equations, whose solution vector $\mathbf{X}$ is defined by the components of vectors $\mathbf{c}$ and $\mathbf{d}$ and the coordinates of points on the boundary portion γ, see also Eq. (15). We point out that due to the ill-posed nature of the inverse problem given by Eqs. (1)–(4), the application of any un-regularized method for the solution of this system of algebraic equations would produce an unstable numerical solution.

4 Numerical results and discussion

We consider the case when the unknown boundary γ is the graph of an unknown Lipschitz function $y : [-r, r] \to \mathbb{R}$, with the x-axis passing through the end points $(-r, 0)$ and $(r, 0)$ of γ and fixing the origin at $x = 0$. In this case, the x-coordinates $x_1^{N_1+1}, x_1^{N_1+2}, \ldots, x_1^N$ of the collocation points $\mathbf{x}^{N_1+1}, \mathbf{x}^{N_1+2}, \ldots, \mathbf{x}^N$ on γ are known. Then the solution vector $\mathbf{X}$ of the system of Eq. (14) depends only upon the vectors $\mathbf{c}$, $\mathbf{d}$ and the y-coordinates of the collocation points on the unknown boundary γ, i.e.,

$$\mathbf{X} = [c_1, c_2, \ldots, c_M, d_1, d_2, \ldots, d_M, x_2^{N_1+1}, x_2^{N_1+2}, \ldots, x_2^N], \tag{15}$$

where $x_2^i = y(x_1^i)$, $i = \overline{(N_1 + 1), N}$.

In order to stabilize the problem, we solve the system of Eq. (14) as an unconstrained optimization problem that consists of minimizing the zeroth-order Tikhonov function

$$F(\mathbf{X}) = \left\| \mathbb{A}(\mathbf{X}) - \mathbf{b}^{\delta} \right\|^2 + \lambda \left\| \mathbf{X} \right\|^2, \tag{16}$$

where $\lambda > 0$ is a regularization parameter to be prescribed and $\mathbf{b}^{\delta} = \mathbf{b} + \boldsymbol{\delta}$ represents the vector $\mathbf{b}$ contaminated by random noise $\boldsymbol{\delta}$. The minimization of (16) imposes $4N_1 + N_2$

equations with $2M+N_2$ unknowns, and for a unique solution we require $2N_1 \geq M$.

When $\lambda = 0$, Eq. (16) becomes the classical nonlinear least-squares function whose minimized solution is unstable since the inverse problem under investigation is ill-posed. The choice of the regularization parameter λ in the functional (16) is crucial for the stability and accuracy of the solution procedure. Various methods have been proposed in the literatures for the choice of this parameter. Among these methods are the discrepancy principle [21] and the L-curve criterion [10]. The L-curve method has been popular for the selection of the regularization parameter, and this works well in many cases. However, in our nonlinear inverse problem we could not obtain an L-curve for the graph of $\|\mathbb{A}(\mathbf{X}) - \mathbf{b}^{\delta}\|$ versus $\|\mathbf{X}\|$ for various values of λ, and this is in agreement with the theoretical results of [26]. Furthermore, the theoretical remarks of [1] show that any heuristic approach which does not assume any a priori knowledge about the amount of noise $\|\boldsymbol{\delta}\|$, such as the L-curve method, is not generally convergent. Therefore, we use the discrepancy principle for a rigorous choice of the regularization parameter λ. This principle consists of plotting the residual norm $\|\mathbb{A}(\mathbf{X}) - \mathbf{b}^{\delta}\|$, as a function of the regularization parameter λ. Then the regularization parameter is chosen as the one for which the residual curve intersects the horizontal line $y = \|\boldsymbol{\delta}\|$. Note that the amount of noise $\|\boldsymbol{\delta}\|$ is required to be known in advance. In order to further justify this choice, we define the accuracy error E as follows:

$$E = \left\{ \sum_{i=N_1+1}^{N} \left[(x_2^i)^{(\text{exact})} - (x_2^i)^{(\lambda)} \right]^2 \right\}^{1/2} \tag{17}$$

and solve the problem for a wide range of positive values of λ. In (17), $(x_2^i)^{(\text{exact})}$ and $(x_2^i)^{(\lambda)}$ are the exact and numerical values, respectively, of the y-coordinates of the boundary γ represented by the graph of the function y. We can then plot the objective function F, given by (16) and the accuracy error E, given by (17), as functions of the regularization parameter λ. Then we expect that the optimal choice of λ returns the smallest values of both F and E. Of course, in the absence of an analytical solution for γ available, the error E cannot be calculated, but it is included herein in order to further justify the optimal choice of the regularization parameter λ given by the discrepancy principle, as it will be illustrated later on in Figs. 6, 7 and 8.

The minimization of the objective functional (16) is performed by using the NAG Fortran library routine E04FCF. This is a comprehensive algorithm for finding an unconstrained minimum of a sum of squares which does not require any derivatives of the objective function to be supplied by the user, these being calculated internally by the routine during the minimization process. The routine uses a combined Gauss-Newton and modified Newton algorithm for this purpose. Further, the routine requires an initial guess to be prescribed, which in this investigation is taken to be 1.0 for the components of the vectors $\mathbf{c}$ and $\mathbf{d}$, and 0.0 for the y-coordinates $(x_2^i)_{i=\overline{(N_1+1),N}}$ of the collocation points on the unknown boundary γ.

In order to illustrate the proposed numerical technique, we assume that, initially, an undamaged material inserted into an engineering environment occupies a circular domain of radius 1 centered at the origin, namely $\Omega_0 = \{(x_1, x_2) |\, x_1^2 + x_2^2 \leq 1\}$. This material subsequently becomes corroded and degenerates into the damaged material occupying a domain Ω. We further assume that the upper semicircular part remains undamaged and it represents the region whose boundary is given by $\Gamma = \{(x_1, x_2) |\, x_1^2 + x_2^2 = 1, x_2 > 0\}$. The part of the boundary that becomes corroded is given by $\gamma = \partial\Omega - \Gamma$. This part of the boundary is unknown, but it remains within the initial configuration of Ω_0. Thus the end points of the corroded and unknown boundary γ are given by $(-1, 0)$ and $(1, 0)$, i.e., $r = 1$.

The analytical solution which satisfies the biharmonic equation (1) is taken as $\psi(x_1, x_2) = x_1^3 + x_2^3$ and the input boundary data (2)–(4) are generated from this solution.

We choose the same numbers of boundary points on the boundary portions Γ and γ, i.e., $N_1 = N_2 = N/2$. It was found, through extensive experimentation, that the choice $M = 40$ source points and $N = 62$ (for Example 1) and $N = 72$ (for Example 2) collocation points gave satisfactorily accurate results. Therefore, this choice was fixed for performing numerical calculations in the inverse boundary detection problem. Further, the $M = 40$ source points were distributed uniformly on a circle around the fixed unit circle domain Ω_0 at a constant distance 1 away from it, i.e., on a circle of radius 2. Of course, it is well-known that the accuracy of the MFS depends on the choice of the pseudo-boundary $\partial\Omega'$ enclosing the solution domain Ω on which the sources are distributed. However, treating the distance between $\partial\Omega'$ and $\partial\Omega$ as an additional parameter to be optimized [25], would complicate even further the difficult inverse and ill-posed problem under investigation and therefore, this analysis is deferred to a future work.

Example 1 First we consider the following simple choice of the exact target for the unknown boundary portion γ:

$$\gamma = \{(x_1, x_2) |\, {x_1}^2 + {x_2}^2 = 1,\ x_2 \leq 0\}. \tag{18}$$

In Fig. 1 we plot the minimum values of the objective function (16), minimized by the NAG routine E04FCF, as a function of the regularization parameter λ, when no noise is introduced in the input boundary data (2) and the exact solution for the unknown boundary γ is given by Eq. (18). From this figure it can be observed that the objective function reaches the smallest value for $\lambda = 10^{-6}$. Therefore, we select this as an optimal choice for the regularization parameter,

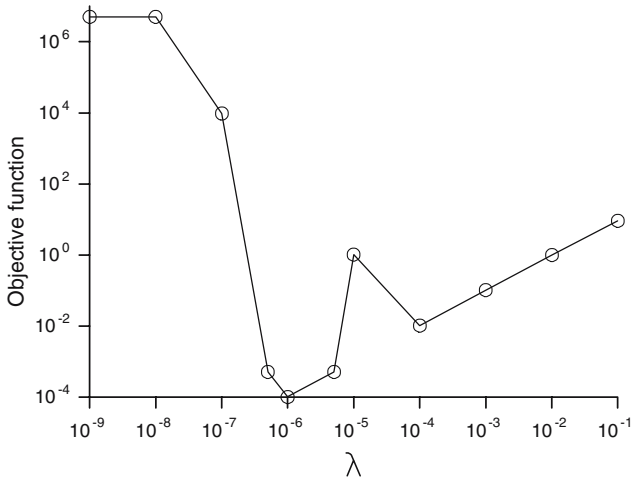

Fig. 1 The minimum values of the objective function F, for various values of the regularization parameter λ, when no noise is introduced in the input boundary data

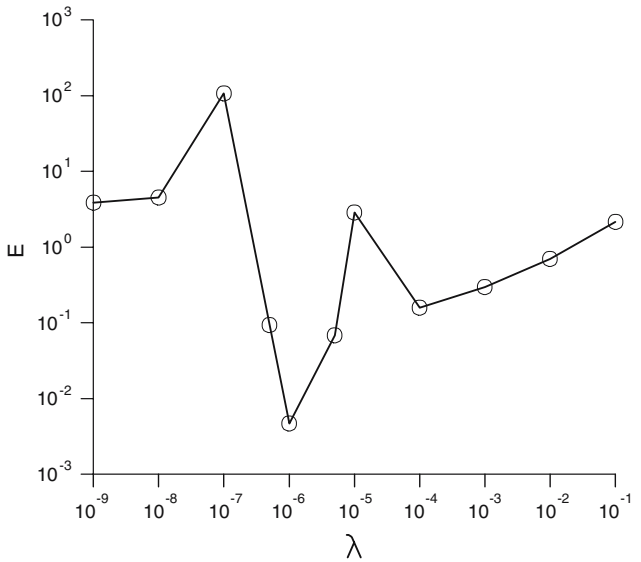

Fig. 2 The accuracy error E, for various values of the regularization parameter λ, when no noise is introduced in the input boundary data

i.e., $\lambda_{\text{opt}} \approx 10^{-6}$. In order to analyze the accuracy of the numerical results for this choice of λ we present, in Fig. 2, the accuracy error E, given by (17), as a function of the regularization parameter λ. From this figure we observe that the smallest value of E also occurs for $\lambda \approx 10^{-6}$.

In order to illustrate the speed of convergence of the optimization procedure we present in Fig. 3 the monotonic decrease of the objective function (16), as a function of the number of iterations for $\lambda = 10^{-6}$. From this figure it can be observed that the objective function decreases quickly in the first ten iterations after which a minimum value of order 10^{-4} is reached.

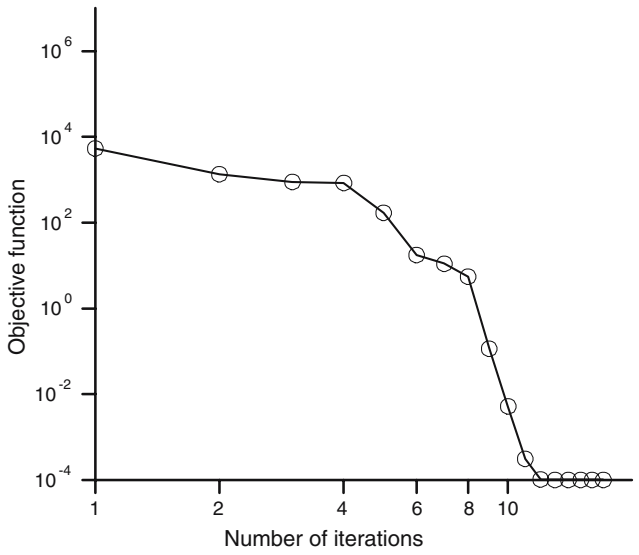

Fig. 3 The convergence of the objective function F, as a function of the number of iterations, when no noise is introduced in the input boundary data and the regularization parameter is fixed at the optimal choice $\lambda_{\text{opt}} = 10^{-6}$

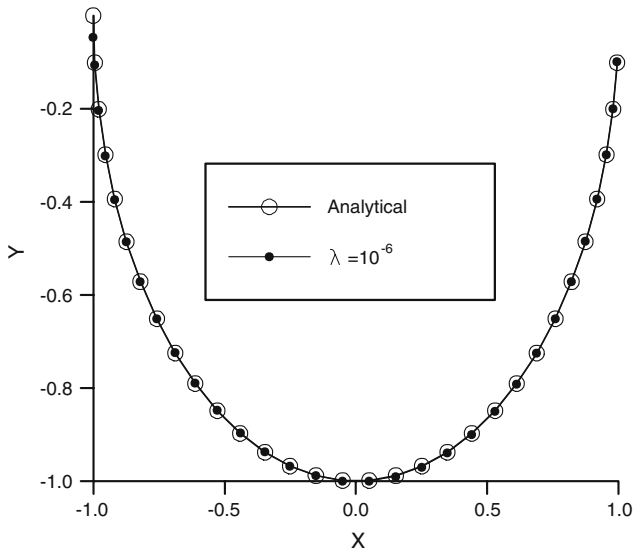

Fig. 4 The boundary γ obtained numerically in comparison with the exact target (18), when no noise is introduced in the input boundary data

Figure 4 shows the boundary γ numerically obtained by using the regularization parameter $\lambda = \lambda_{\text{opt}} = 10^{-6}$, when no noise is introduced in the input boundary data, in comparison with its exact target given by Eq. (18). From this figure it can be observed that the numerical results are stable and their agreement with the exact solution is excellent.

In order to further analyze the optimal choice of the regularization parameter, we present in Fig. 5 the numerical solution for the unknown boundary γ for various values of the regularization parameter $\lambda \in \{10^{-8}, 10^{-7}, 10^{-6}, 5 \times 10^{-6}\}$

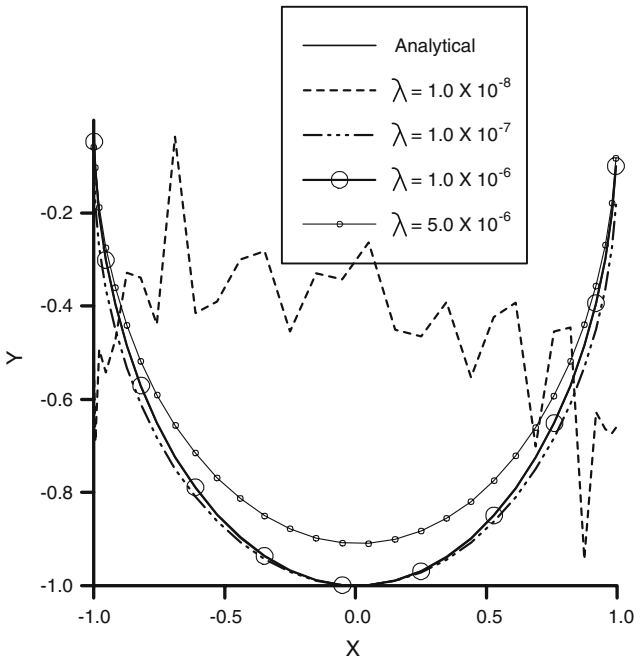

Fig. 5 The boundary γ obtained numerically, for various values of the regularization parameter $\lambda \in \{10^{-8}, 10^{-7}, 10^{-6}, 5 \times 10^{-6}\}$, when no noise is introduced in the input boundary data

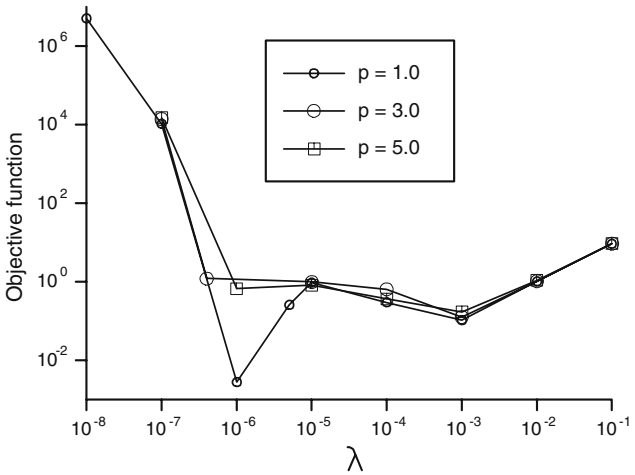

Fig. 6 The minimum values of the objective function F, for various values of the regularization parameter λ, when 1, 3 and 5% noises are introduced in the input data φ

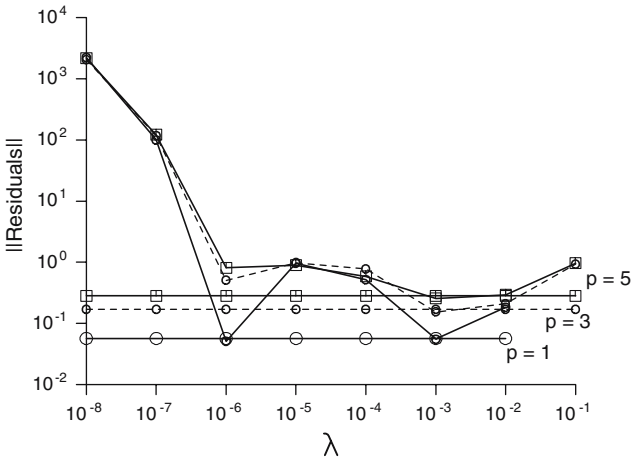

Fig. 7 The norms of the residuals $\|\mathbb{A}(\mathbf{X}) - \mathbf{b}^{\delta}\|$, for various values of the regularization parameter λ, when 1, 3 and 5% noises $\|\boldsymbol{\delta}\|$ (*horizontal lines*) are introduced in the input data φ

selected in close vicinity of the optimal choice $\lambda_{\text{opt}} = 10^{-6}$, when no noise is present in the input boundary data. The exact solution for the unknown boundary γ given by Eq. (18) is also included in the figure. From this figure it can be observed that the numerical solution for the unknown boundary γ is unstable and largely inaccurate for $\lambda = 10^{-8}$. The solution becomes stable and reasonably accurate for $\lambda = 10^{-7}$. Moreover, excellent agreement of the numerical solution with the exact solution is observed for $\lambda = 10^{-6}$, see also Fig. 4. The solution retains its stable nature for $\lambda = 5 \times 10^{-6}$ with slightly increased inaccuracy. Therefore, we conclude that the numerical solution for the unknown boundary γ is stable and accurate if the regularization parameter λ is chosen according to the discrepancy principle. Otherwise, if λ is chosen too large the numerical solution becomes inaccurate, whilst if λ is chosen too small the numerical solution becomes unstable.

Next, in order to simulate the errors inherently present in any practical measurement, we perturb the data φ in (2) with random noise δ such that $\varphi^{\delta} = \varphi + \delta$. We generate this noise δ by using the NAG routine G05DDF with mean zero and standard deviation $\sigma = \frac{p}{100} \times \max_{\Gamma} |\varphi|$ and choose $p \in \{1, 3, 5\}$ to test stability of the solution when 1, 3 and 5% noises are introduced in the function φ.

Figure 6 shows the minimum values of the objective functional (16), minimized by the NAG routine E04FCF, as a function of the regularization parameter λ, when $p\% = 1$, 3 and 5% random noises are introduced in the function φ. From this figure, we observe that for $p\% = 1\%$ the smallest value of the objective function is obtained for $\lambda = 10^{-6}$, approximately. Figure 6 also illustrates that the value of the objective function is the smallest for $\lambda = 10^{-3}$, when 3 and 5% noises are introduced in the function φ.

In order to use the discrepancy principle for the selection of λ_{opt}, we present in Fig. 7 the norms of the residuals $\|\mathbb{A}\mathbf{X} - \mathbf{b}^{\delta}\|$, for various values of the regularization parameter λ, when 1, 3 and 5% noises $\|\boldsymbol{\delta}\|$ are introduced in the input data φ. From Fig. 7, we can identify two values for the optimal choice of the regularization parameter when φ contains 1% random noise. These optimal values are $\lambda = 10^{-6}$ and 10^{-3}. However, as it can be observed from Fig. 6, the minimum value of the objective functional is the smallest for $\lambda = 10^{-6}$. Therefore, we choose this as an optimal value of

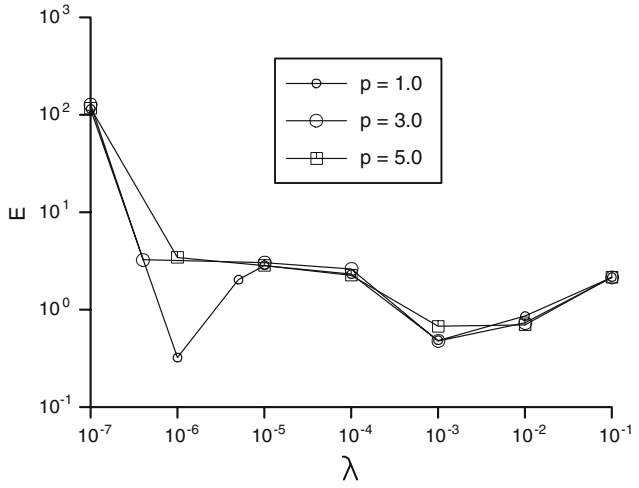

Fig. 8 The accuracy error E, for various values of the regularization parameter λ, when 1, 3 and 5% noises are introduced in the input data φ

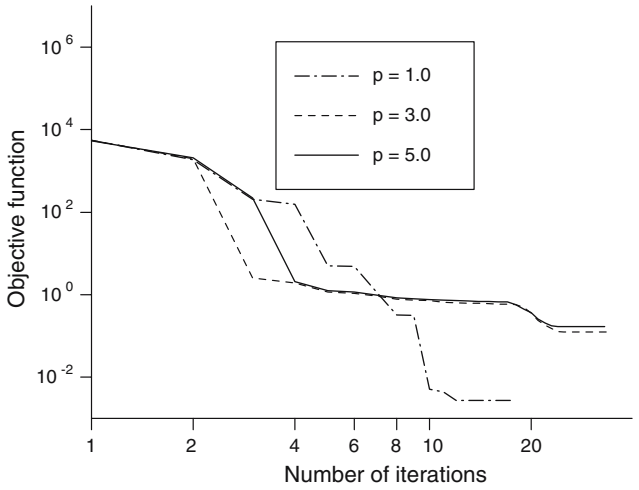

Fig. 9 The convergence of the objective function F, as a function of the number iterations, when 1, 3 and 5% noises are introduced in the input data φ and the regularization parameter is fixed at the optimal choice λ_{opt}

the parameter λ when $p = 1$. Similarly, using Figs. 6 and 7 we choose $\lambda_{\text{opt}} = 10^{-3}$ when the data φ contains 3 and 5% noises.

As before, in the no noise case, the optimal choice of the regularization parameter, when the input data φ contains 1, 3 and 5% noises, is further justified by presenting in Fig. 8, the accuracy error E, as a function of λ. From this figure it can be seen that the smallest value of the accuracy error E occurs at the same value of $\lambda = \lambda_{\text{opt}}$ as that given by the discrepancy principle shown in Fig. 7.

Figure 9 shows the objective function (16), as a function of the number of iterations for various $p \in \{1, 3, 5\}$ and the regularization parameter λ fixed at its optimal choice given by

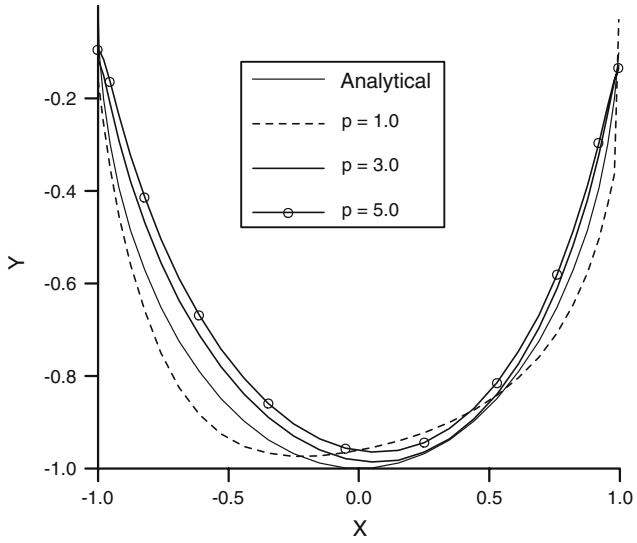

Fig. 10 The boundary γ numerically obtained in comparison with the exact target γ given by Eq. (18), when 1, 3 and 5% noises are introduced in the input data φ and the regularization parameter is fixed at the optimal choice λ_{opt}

Figs. 6 and 7. From this figure it can be seen that the objective functional decreases very quickly and approaches its smallest value after a small number of iterations; in fact less than 25. This shows high efficiency of the proposed optimization technique.

Figure 10 shows the boundary γ numerically obtained for $\lambda = \lambda_{\text{opt}}$ in comparison with its exact target given by Eq. (18), when the input data φ is corrupted by 1, 3 and 5% random noise. From this figure we observe that, for all levels of noise, the numerically retrieved solution is stable and consistent with the amount of noise introduced in the input data φ. Moreover, the numerical solution converges to the exact solution as the amount of noise decreases to zero.

Example 2 We now consider the retrieval of a complicated boundary that changes its concavity. This consists of the union of the three boundary portions γ_1, γ_2 and γ_3, i.e.,

$$\gamma = \bigcup_{i=1}^{3} \gamma_i, \tag{19}$$

where γ_1, γ_2 and γ_3 are given by

$$\gamma_1 = \{(x_1, x_2) |\ (x_1 - 1/3)^2 + x_2^2 = 1/9,\ x_2 \leq 0\}, \tag{20}$$

$$\gamma_2 = \{(x_1, x_2) |\ x_1^2 + x_2^2 = 1/9,\ x_2 \geq\ 0\}, \tag{21}$$

$$\gamma_3 = \{(x_1, x_2) |\ (x_1 + 1/3)^2 + x_2^2 = 1/9,\ x_2 \leq 0\}. \tag{22}$$

Using the scheme detailed in the previous example, we choose $\lambda_{\text{opt}} = 10^{-6}$, 10^{-4} and 3×10^{-4}, when the data φ is perturbed by 0, 3 and 5% random noises. Figure 11 shows the numerical solution for the unknown boundary γ for these optimal values of the regularization parameter. Also included in this figure is the corresponding exact solution (19)–(22) of

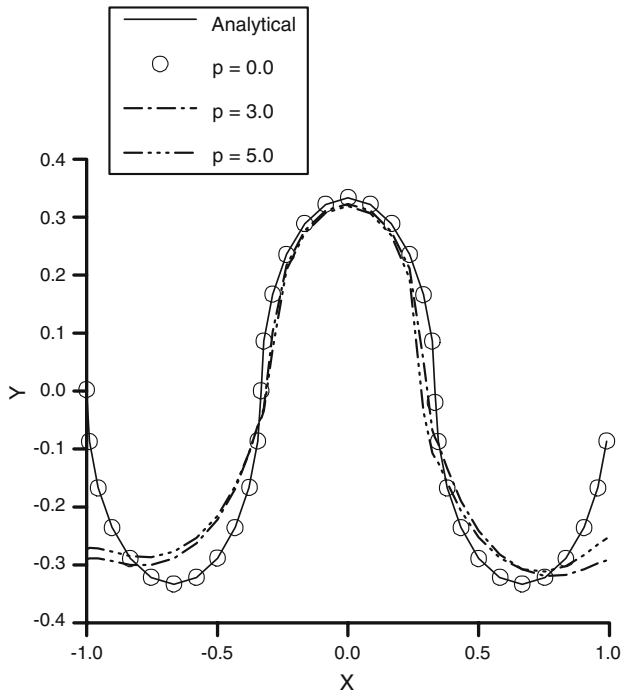

Fig. 11 The boundary γ numerically obtained in comparison with the exact target γ given by Eqs. (19)–(22), when 0, 3 and 5% noises are introduced in the input data φ

the boundary portion γ. From this figure it can be seen that the numerical solution remains stable and consistent with the amount of noise included in the input data φ. Further, the solution converges to the exact solution as the amount of noise decreases to zero.

5 Conclusions

A nonlinear inverse problem associated to the biharmonic equation has been investigated numerically using the method of fundamental solutions (MFS). This problem requires the determination of an unknown boundary portion of a solution domain from additional Cauchy data on the remaining part of the boundary. The problem of solving the resulting system of nonlinear equations was reformulated as an optimization problem that minimizes the norm of the least-squares residual. It was found that this minimization procedure produces an inaccurate and unstable numerical solution when regularization is not included. Therefore, the Tikhonov zeroth-order regularization was included in the proposed numerical algorithm to overcome this difficulty. The regularized MFS numerical algorithm, with an optimal choice of the regularization parameter based on the discrepancy principle, produces an accurate numerical solution for the unknown boundary that is stable under small changes in the input boundary data.

Acknowledgments The first author, A. Zeb, gratefully acknowledges the financial support of the Higher Education Commission of Pakistan. The comments and suggestions made by the referees are gratefully acknowledged.

References

1. Bakushinskii AB (1985) Remarks on choosing a regularization parameter using the quasioptimality and ratio criterion. USSR Comput Maths Math Phys 24:181–182
2. Balakrishnan K, Ramachandran PA (1999) A particular solution Trefftz method for non-linear Poisson problems in heat and mass transfer. J Comput Phys 150:239–267
3. Balakrishnan K, Ramachandran PA (2001) Osculatory interpolation in the method of fundamental solutions for nonlinear Poisson problems. J Comput Phys 172:1–18
4. Chen CS, Golberg MA, Hon YC (1998) The method of fundamental solutions and quasi-Monte Carlo method for diffusion equations. Int J Numer Methods Eng 43:1421–1436
5. Chen CW, Young DL, Tsai CC, Murugesan K (2005) The method of fundamental solutions for inverse 2D Stokes problems. Comput Mech 37:2–14
6. Cho HA, Golberg MA, Muleshkov AS, Li X (2004) Trefftz method for time dependent partial differential equations. Comput Mat Cont 1:1–37
7. Fairweather G, Karageorghis A (1998) The method of fundamental solutions for elliptic boundary value problems. Adv Comput Math 9:69–95
8. Golberg MA (1995) The method of fundamental solutions for Poisson's equation. Eng Anal Bound Elem 16:205–213
9. Golberg MA, Chen CS (1996) Discrete projection methods for integral equations. Comput Mech Publ Southampton
10. Hansen PC (1998) Rank-deficient and discrete ill-posed problems: numerical aspects of linear inversion. SIAM, Philadelphia
11. Karageorghis A (2001) The method of fundamental solutions for calculation of the eigenvalues of the Helmholtz equation. Appl Math Lett 14:837–842
12. Karageorghis A, Fairweather G (1987) The method of fundamental solutions for the numerical solution of the biharmonic equation. J Comput Phys 69:434–459
13. Karageorghis A, Fairweather G (1988) The Almansi method of fundamental solutions for solving biharmonic problems. Int J Numer Meth Eng 26:1665–1682
14. Karageorghis A, Fairweather G (1989) The simple layer potential method of fundamental solutions for certain biharmonic problems. Int J Numer Meth Fluids 9:1221–1234
15. Kupradze VD, Aleksidze MA (1964) The method of functional equations for approximate solution of certain boundary value problems. USSR Comput Maths Math Phys 4:82–126
16. Lesnic D, Berger JR, Martin PA (2002) A boundary element regularization method in potential corrosion damage. Inverse Problems Eng 10:163–182
17. Marin L (2006) Numerical boundary identification for Helmholtz-type equations. Comput Mech 39:25–40
18. Marin L, Lesnic D (2005) The method of fundamental solutions for inverse boundary value problems associted with the two dimentional biharmonic equation. Math Comput Model 42:261–278
19. Mathon R, Johnston RL (1977) The approximate solution of elliptic boundary value problems by fundamental solutions. SIAM J Numer Anal 14:638–650
20. Mera NS, Lesnic D (2005) A three-dimensional boundary determination problem in potential corrosion damage. Comput Mech 36:129–138

21. Morozov VA (1966) On the solution of functional equations by the method of regularization. Soviet Math Dokl 7:414–417
22. Poullikkas A, Karageorghis A, Georgiou G (1998) Method of fundamental solutions for harmonic and biharmonic boundary value problems. Comput Mech 21:416–423
23. Ramm AG (1988) An inverse problem for biharmonic equation. Internat J Math Math Sci 11:413–415
24. Schaefer PW (1974) On existence in the Cauchy problem for the biharmonic equation. Compos Math 28:203–207
25. Tankelevich R, Fairweather G, Karageorghis A, Smyrlis Y-S (2006) Potential field based geometric modelling using the method of fundamental solutions. Int J Numer Methods Eng 68:1257–1280
26. Vogel C (1996) Non-convergence of the L-curve regularization parameter selection method. Inverse Problems 12:535–547
27. Young DL, Tsai CC, Murugesan K, Fan CM, Chen CW (2004) Time-dependent fundamental solutions for homogeneous diffusion problems. Eng Anal Bound Elem 28:1463–1473
28. Young DL, Hu SP, Chen CW, Fan CM, Murugesan K (2005) Analysis of elliptical waveguides by the method of fundamental solutions. Micro Opt Tech Lett 44:552–558
29. Young DL, Chen CW, Fan CM, Murugesan K, Tsai CC (2005) Method of fundamental solutions for Stokes flows in a rectangular cavity with cylinders. Eur J Mech B Fluids 24:703–716
30. Young DL, Chiu CL, Fan CM, Tsai CC, Lin YC (2006) Method of fundamental solutions for multidimensional Stokes equations by the dual-potential formulation. Eur J Mech B Fluids 25:877–893
31. Young DL, Jane SJ, Fan CM, Murugesan K, Tsai CC (2006) The method of fundamental solutions for 2D and 3D Stokes problems. J Comput Phys 211:1–8